Title
Optical Doppler tomographic imaging of fluid flow velocity in highly scattering media.

Journal
Optics Letters, 22(1)

ISSN
0146-9592

Authors
Chen, Zhongping
Milner, Thomas E
Dave, Digant
et al.

Publication Date
1997

DOI
10.1364/ol.22.000064

Optical Doppler tomographic imaging of fluid flow velocity in highly scattering media

Zhongping Chen, Thomas E. Milner, Digant Dave, and J. Stuart Nelson

Beckman Laser Institute and Medical Clinic, University of California, Irvine, Irvine, California 92715

Received August 26, 1996

An optical Doppler tomography (ODT) system that permits imaging of fluid flow velocity in highly scattering media is described. ODT combines Doppler velocimetry with the high spatial resolution of low-coherence optical interferometry to measure fluid flow velocity at discrete spatial locations. Tomographic imaging of particle flow velocity within a circular conduit submerged 1 mm below the surface in a highly scattering phantom of Intralipid is demonstrated. © 1997 Optical Society of America

Accurate determination of location and flow velocity of moving particles in highly scattering media is important for medical diagnostics. Detailed knowledge of *in vivo* blood flow under the skin surface, for example, is essential for burn-depth determination, laser treatment of port wine stains, and photodynamic therapy.[1–3] We previously reported application of a conventional fiber-optic Michelson interferometer that uses a superluminescent diode (SLD) light source to determine the flow velocity of polystyrene beads in a turbid conduit with a detection volume as small as 5 μm × 5 μm × 15 μm.[4] In this Letter we describe an optical Doppler tomography (ODT) system that permits imaging of fluid flow velocity within a circular conduit submerged 1 mm below the surface in a scattering phantom of intralipid.

ODT combines Doppler velocimetry with optical coherence tomography (Fig. 1). Optical coherence tomography is an imaging technique that uses a low-coherence Michelson interferometer to perform optical sections of biological materials.[5] The amplitude of the backscattered light is determined by measurement of the interference fringe intensity generated between the reference and the target arms. High axial spatial resolution is possible because interference is observed only when the optical path lengths of light in the target and the reference arms match to within the source coherence length.

ODT makes use of the principle that the frequency of light scattered from a moving particle is Doppler shifted (Δf) according to

$$\Delta f = \frac{1}{2\pi}(\mathbf{k}_s - \mathbf{k}_i)\cdot\mathbf{V}, \tag{1}$$

where $\mathbf{k}_i$ and $\mathbf{k}_s$ are wave vectors of incoming and scattered light, respectively, and $\mathbf{V}$ is the velocity vector of the moving particles. In an ODT system only backscattered light is detected. Given the angle (θ) between the target beam in air and the flow direction, the Doppler shift [Eq. (1)] is simplified to

$$\Delta f = 2V\cos(\theta)/\lambda_0, \tag{2}$$

where λ_0 is the vacuum center wavelength of the target beam. When light backscattered from a moving particle interferes with the reference beam, beating at the Doppler frequency occurs, shifting the frequency of the interference fringe intensity from that of the optical phase modulation. The sign of the frequency shift (Δf) depends on the direction of flow; the frequency shift is positive when the angle between ($\mathbf{k}_s - \mathbf{k}_i$) and $\mathbf{V}$ is less than 90° and negative when the angle is greater than 90°. When the angle θ is known, detection of the Doppler frequency shift (Δf) permits measurements of the particle flow velocity at discrete spatial locations.

In our ODT system a SLD (λ_0 = 850 nm, $\Delta\lambda$ = 25 nm, P = 1 mW) is used as the low-coherence source. Light from the SLD and an aiming beam (He–Ne laser, λ = 633 nm) is coupled into a fiber-optic Michelson interferometer by a 2 × 1 coupler. SLD light is split into reference and target arms of the interferometer by a 2 × 2 (50:50) fiber coupler. Stress birefringence is used to match the polarization of reference and sample beams and to optimize fringe contrast. The optical path lengths of light in the reference and the target arms are modulated (1600 Hz) with piezoelectric cylinders electrically driven by a ramp waveform. The target arm is tilted 75° with respect to the direction of flow. Light in the target arm is focused onto the sample with a gradient-

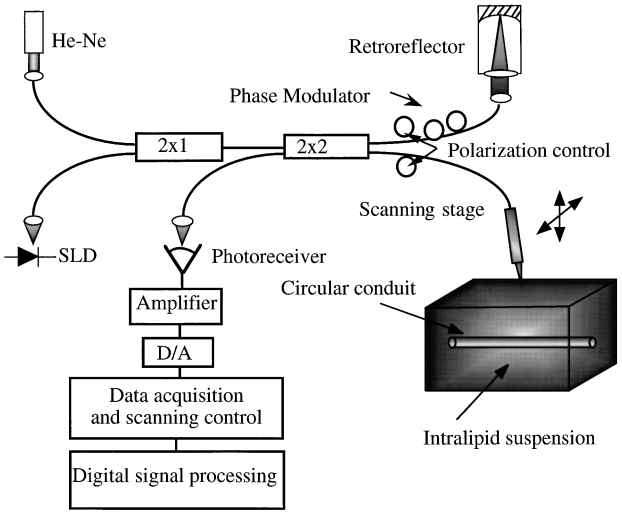

Fig. 1. Schematic diagram of optical Doppler tomography system. D/A, digital-to-analog converter.

0146-9592/97/010064-03$10.00/0

index lens (N.A. = 0.2). Two-dimensional images are formed by sequential lateral scans at a constant horizontal velocity of 800 μm/s, followed by an incremental probe movement in a vertical (axial) direction. To maintain a zero optical path-length difference between the beam waist in the sample and the reference mirror, we use a dynamic focus tracking method. In this approach, for each incremental axial probe movement (δ_1) the reference mirror is moved (δ_2) to compensate for the new position of the beam waist in the sample. The relationship between δ_1 and δ_2 can be derived from geometrical optics:

$$\delta_2 = (\overline{n}^2 - 1)\delta_1 , \tag{3}$$

where $\overline{n}$ is the mean sample refractive index. Light backscattered from the sample recombines with the reference beam within the 2 × 2 coupler and interferes only when the optical path-length difference is less than or equal to the coherence length of the SLD light. Optical interference fringe intensity is measured by a silicon photovoltaic receiver. The signal is digitized with a 16-bit analog–digital converter and transferred to a computer workstation for processing. The interference fringe intensity at each pixel is transformed by a fast-Fourier-transform algorithm. A tomographic structural image is obtained by calculation of the power in the Fourier component corresponding to the phase-modulation frequency. Fluid flow velocity at each pixel is determined by measurement of the Doppler frequency shift, which is obtained by calculation of the difference between the centroid of the measured frequency spectrum at each pixel and the phase-modulation frequency. The lateral and the axial spatial resolution are limited by the beam spot size (5 μm) and the coherence length of the source (15 μm), respectively. The velocity resolution depends on the angle between the flow velocity and the probe beam, and the duration of interference fringe data is recorded at each pixel. It is approximately 100 μm/s for our setup and can be improved if a larger angle and (or) a longer acquisition time is used.

For a demonstration particle flow imaging in a scattering medium, two models are under study. The first model uses a circular-section polyethylene conduit containing a suspension of polystyrene beads (diameter 1.7 μm, concentration 3.7 × 10^5/mm^3) all submerged in a phantom of 0.25% Intralipid solution. The inner and outer diameters of the polyethylene conduit are 580 and 960 μm, respectively. The second model uses the same circular conduit containing a moving suspension of 1% Intralipid, all submerged in a phantom of 1% intralipid solution.

Results from the first model containing moving polystyrene beads in a circular conduit submerged in a phantom of Intralipid solution are shown in Fig. 2. Figure 2A is the recorded tomographic image with static beads. The backscattered light intensity from the phantom is color coded, with red and green representing high and low reflectivity, respectively. The color change from red at the surface to green at the bottom indicates strong attenuation of the probe beam by the phantom. The dynamic range of the measured

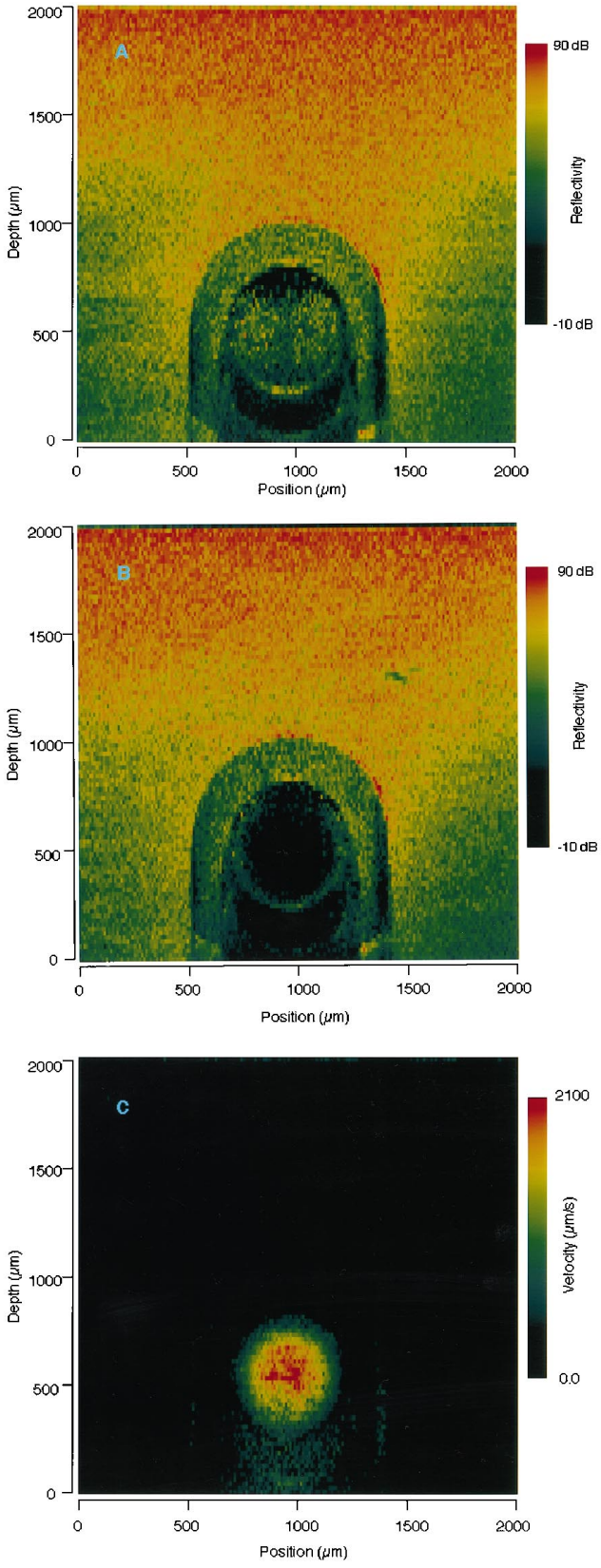

Fig. 2. ODT image of polystyrene beads (diameter 1.7 μm; concentration 3.7 × 10^5/mm^3) in a 580-μm-diameter polyethylene conduit submerged 1 mm below the surface in a scattering phantom of 0.25% Intralipid suspension. A, tomographic image of static polystyrene beads; B, tomographic image of flowing polystyrene beads; C, velocity image of flowing beads.

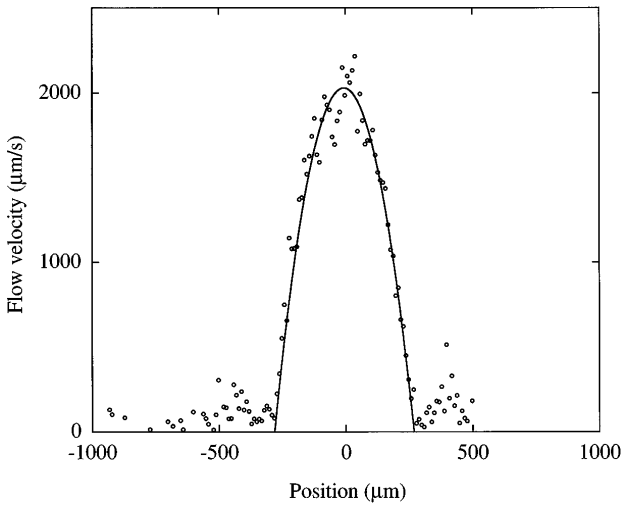

Fig. 3. Horizontal cross section of the velocity profile at the center of the conduit. The open circles are the experimental data and the solid curve is a theoretical fit, assuming laminar flow. The agreement between the two suggests laminar flow, as expected.

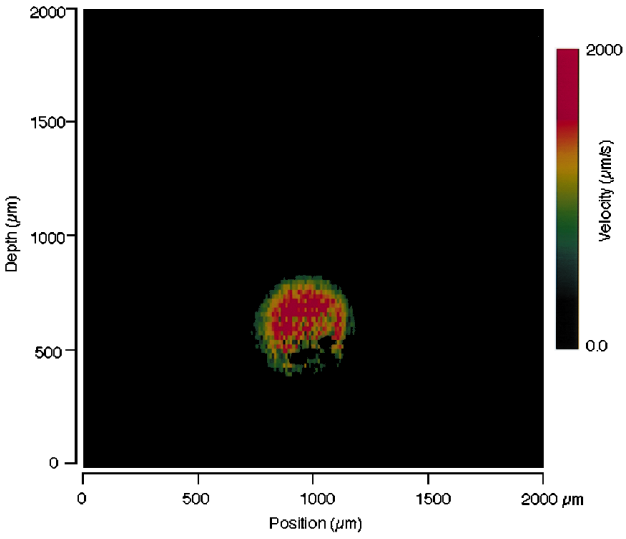

Fig. 4. ODT images of flowing 1% Intralipid in a circular conduit submerged 1 mm below the surface in a scattering phantom of 1% Intralipid solution.

backscattered light in the tomographic structural image is greater than 100 dB. Backscattered light from both the beads and the conduit wall is evident in this image. The depth of the top surface of the conduit is at 1 mm below the surface of the phantom. When beads are flowing through the conduit (Fig. 2B), all features of the image remain unchanged, except that the area within the circular conduit appears dark. This effect is due to flowing beads that shift the interference fringe frequency away from the phase-modulation frequency. Figure 2C is the tomographic velocity image of the flowing beads, where features are color coded with red and black for high (2100-μm/s) and zero velocity, respectively. Static regions in the conduit appear dark ($V = 0$), whereas the presence of beads moving at different velocities is evident. Beads near the center of the conduit are observed to move faster than those near the circular wall. A horizontal cross section of the velocity profile at the center of the conduit is shown in Fig. 3, in which the open circles are the experimental data and the solid curve is a theoretical fit, assuming laminar flow with a known conduit inner diameter. Agreement between theory and experiment suggests laminar flow, as expected.

In the second model, 1% Intralipid flowing through the conduit submerged in a highly scattering phantom is tested to demonstrate the potential applications of ODT for measuring fluid particle velocity in biological tissues. A tomographic image of flow velocity is shown in Fig. 4, in which the image is color coded with red and black for high (2000-μm/s) and zero velocity, respectively. Although scattering from the Intralipid is high ($\mu_s = 23$ cm^{-1}) and the conduit as viewed from the top surface of the phantom is invisible to the unaided eye, the presence of beads flowing at different velocities is evident in the ODT image. These findings demonstrate that ODT is capable of detecting flow submerged in highly scattering media similar to biological tissue. Because the data are obtained in a single scan, ODT permits tomographic imaging of both structural features and fluid flow velocity simultaneously. Given the noninvasive nature of the measurement, relatively compact size, and simple hardware requirements of the system, ODT may find a number of biomedical applications in which locating and monitoring blood flow is essential.

We thank M. J. C. van Gemert, B. Tromberg, X. J. Wang, and D. J. Smithies for helpful discussions. Results of this research were presented at the Gordon Conference on Lasers in Medicine and Biology (June 1996). Independent flow imaging in less-turbulent media ($\mu_S = 0.3$ cm^{-1}) was also described by Izatt *et al.*[6] This project is supported by research grants from the Biomedical Research Technology Program and the Institute of Arthritis and Musculoskeletal and Skin Diseases (1R29-AR41638-01A1 and 1R01-AR42437) at the National Institutes of Health, the Whitaker Foundation, and the Dermatology Foundation. Institute support from the U.S. Department of Energy, the National Institutes of Health, and the Beckman Laser Institute Endowment is also gratefully acknowledged.

References

1. Z. B. M. Niazi, T. J. H. Essex, R. Papini, D. Scott, N. R. Mclean, and M. J. M. Black, Burns **19,** 485 (1993).
2. J. S. Nelson and J. Applebaum, Clin. Pediatr. (Philadelphia) **29,** 503 (1990).
3. M. Korbelik and G. Krosl, Br. J. Cancer **70,** 604 (1994).
4. X. J. Wang, T. E. Milner, and J. S. Nelson, Opt. Lett. **20,** 1337 (1995).
5. D. Huang, E. A. Swanson, C. P. Lin, J. S. Schuman, W. G. Stinson, W. Chang, M. R. Hee, T. Flotte, K. Gregory, C. A. Puliafito, and J. G. Fujimoto, Science **254,** 1178 (1991).
6. J. Izatt and M. Kukarni, in *Conference on Lasers and Electro-Optics,* Vol. 9 of 1996 OSA Technical Digest Series (Optical Society of America, Washington, D.C., 1996), postdeadline paper CPD3-1.